Atmos. Chem. Phys. Discuss., doi:10.5194/acp-2017-44, 2017
Manuscript under review for journal Atmos. Chem. Phys.
Discussion started: 8 February 2017

Atmospheric Chemistry and Physics Discussions

Comparison of primary and secondary particle formation from natural gas engine exhaust and of their volatility characteristics

Jenni Alanen[1], Pauli Simonen[1], Sanna Saarikoski[2], Hilkka Timonen[2], Oskari Kangasniemi[1], Erkka Saukko[1], Risto Hillamo[2], Kati Lehtoranta[3], Timo Murtonen[3], Hannu Vesala[3], Jorma Keskinen[1], and Topi Rönkkö[1]

[1]Aerosol Physics, Faculty of Natural Sciences, Tampere University of Technology, P.O. Box 692, 33101 Tampere, Finland
[2]Atmospheric Composition Research, Finnish Meteorological Institute, P.O. Box 503, 00101 Helsinki, Finland
[3]VTT Technical Research Centre of Finland Ltd., P.O. Box 1000, 02044 VTT, Espoo, Finland

Correspondence to: Topi Rönkkö (topi.ronkko@tut.fi)

Abstract. Natural gas usage in traffic and energy production sector is a growing trend worldwide, thus an assessment of its effects on air quality, human health and climate is required. Engine exhaust is a source of primary particulate emissions and secondary aerosol precursors that both contribute to air quality and can cause adverse health effects. Technologies, such as cleaner engines or fuels, that produce less primary and secondary aerosol could potentially significantly decrease the atmospheric particle concentrations and their adverse effects. In this study, we used a potential aerosol mass (PAM) chamber to investigate the secondary aerosol formation potential of natural gas engine exhaust. The PAM chamber was used with a constant UV-light voltage that resulted in an equivalent atmospheric age of 11 days at a maximum. The studied passenger car engine, retrofitted to run with natural gas, was observed to have a low or moderate secondary particle formation potential, although the simulated atmospheric ages were relatively long. The secondary organic aerosol (SOA) formation potential was measured to be 8-18 mg kg_{fuel}^{-1}. However, the mass of total aged particles, i.e. particle mass measured downstream the PAM chamber, was 6-184 times as high as the mass of the emitted primary exhaust particles. The total aged particles consisted mainly of nitrate, organic matter, sulfate and ammonium, the fractions depending on exhaust after-treatment and used engine parameters. Also the volatility, composition and concentration of the total aged particles were found to depend on the engine operating mode, catalyst temperature and catalyst type. For example, a high catalyst temperature promoted the formation of sulfate particles, whereas a low catalyst temperature promoted nitrate formation. However, especially the concentration of nitrate needed a long time, more than half an hour, to stabilize, which complicated the conclusions but also indicates the sensitivity of nitrate measurements on experimental parameters such as emission source and system temperatures. Sulfate was measured to have the highest evaporation temperature and nitrate the lowest. The evaporation temperature of ammonium depended on the fractions of nitrate and sulfate in the particles. The average volatility of the total aged particles was measured to be lower than that of primary particles, indicating better stability of the aged natural gas engine emitted aerosol in the atmosphere. According to the results of this study, the shift from traditional liquid fuels to natural gas can have a decreasing effect on total particle pollution in the atmosphere; in addition to the very low primary particle emissions, also the secondary organic aerosol formation potential of natural gas exhaust is lower or on the same level as the SOA formation potential measured on liquid fuels in previous studies.

Atmos. Chem. Phys. Discuss., doi:10.5194/acp-2017-44, 2017
Manuscript under review for journal Atmos. Chem. Phys.
Discussion started: 8 February 2017

Atmospheric Chemistry and Physics Discussions

1 Introduction

Primary aerosol particles are emitted directly into the atmosphere by various anthropogenic sources, such as vehicles, engines or power plants, and biogenic sources. Secondary aerosol particle mass forms during the atmospheric oxidation of emitted precursor gases. In this process, the saturation vapor pressure of the organic and inorganic gases becomes lower thus allowing them to transfer into particle phase by condensation and nucleation (Hallquist et al., 2009; Murphy et al., 2014). In addition to biogenic sources, also traffic and other anthropogenic sources are contributors to secondary aerosol formation (Kanakidou et al., 2005).

Fine particles (<2.5 μ m) are found to cause people adverse health effects and premature mortality (Dockery and Pope III, 1994; Lelieveld et al., 2015). The relative contribution of primary and secondary particles on the health effects is still unknown, but there are indications that secondary particles can be even more hazardous than primary particles (Künzi et al., 2015; McWhinney et al., 2011; Rager et al., 2011). Therefore, both primary and secondary particle emissions must be taken into consideration when evaluating the health effects of particle emissions.

Aerosols play an important role in climate as well. Fine particles in the atmosphere affect the radiative balance of the atmosphere by either warming or cooling it depending on their properties (Myhre et al., 2013) but large uncertainties remain in the contribution of particles to climate change or its prevention. Clouds contribute to the radiative balance of the atmosphere, too. Aging of an aerosol can lead to increased hygroscopicity of the particles (Kanakidou et al., 2005) and a higher likelihood that they act as cloud condensation nuclei. The preservation and lifetime of the particles in the atmosphere partly define how large their impact is on climate.

The formation process of secondary inorganic aerosol can be modeled rather accurately because the number of different inorganic precursors is small and their oxidation reactions are well known. Secondary organic aerosol (SOA) is a more complex subject area due to the vast amount of different organic compounds, their potential reactions and the still unknown participation of all compounds in secondary aerosol formation (Hallquist et al., 2013; Jimenez et al., 2009). Hence, SOA has been a hot topic in aerosol science during the past decade (Huang et al., 2014; Robinson et al., 2007; Virtanen et al., 2010). However, also the relative fractions of secondary organic and inorganic aerosol from various emission sources still need to be studied. Both secondary organic and secondary inorganic aerosol can significantly contribute to air quality deterioration (Huang et al., 2014).

Particle number and mass emission regulations for combustion engines have decreased the primary particle emissions from vehicles, especially the emissions from diesel vehicles. Secondary particle precursor emissions or secondary aerosol formation potential are not directly regulated but some of the current emission regulations affect secondary particle precursor emissions indirectly. For instance, oxidative exhaust after-treatment devices reduce the total hydrocarbon emissions and thus probably the emissions of secondary organic aerosol precursors but simultaneously also change the oxidation state of inorganic compounds. In general, vehicles emit substantial amounts of precursors for SOA formation, so that the amount of potential SOA often exceeds the emissions of primary organic aerosol. For instance, gasoline vehicles emit 9-15 times or even two orders of magnitude higher secondary organic particulate matter than primary organic particle mass (Karjalainen et al., 2016; Nordin et al., 2013; Platt et al., 2013; Tkacik et al., 2014). Indeed, Bahreini et al. (2012) found that gasoline engine originated secondary

Atmos. Chem. Phys. Discuss., doi:10.5194/acp-2017-44, 2017
Manuscript under review for journal Atmos. Chem. Phys.
Discussion started: 8 February 2017

Atmospheric Chemistry and Physics Discussions

organic aerosol forms the majority of the SOA in and downwind of large metropolitan areas. From diesel vehicles without a particle filter, SOA mass formation potential is of the same magnitude as the primary particle mass emission (Weitkamp et al., 2007).

Exhaust after-treatment can reduce the secondary aerosol formation potential from engine exhaust, especially the SOA formation potential. In general, diesel fuel has the strongest secondary organic aerosol formation potential amongst diesel, jet fuel, gasoline and Fischer-Tropsch from natural gas and coal (Jathar et al., 2013). However, diesel vehicles equipped with oxidation catalysts or catalytic particle filters have been reported to be minor secondary particle emitters (Chirico et al., 2010; Gordon et al., 2014b; Samy and Zielinska, 2010). In gasoline engines, too, functioning exhaust after-treatment can reduce the secondary particle formation clearly (Karjalainen et al., 2016). The secondary aerosol precursor emission of engines and vehicles are also strongly depended on the driving conditions which should be taken into account in emission comparisons.

For instance, Tkacik et al. (2014) showed that the secondary inorganic mass often exceeds the amount of the secondary organic aerosol in a highway tunnel, even by a factor of two. The main contributor to secondary inorganic aerosol in their study was ammonium nitrate that originates from NO_x and ammonia emissions. According to the study of Karjalainen et al. (2016), large fractions of nitrate in the secondary inorganic particles is characteristic for highway driving and the inorganic species concentrations are relatively low when compared to secondary organic aerosol formed during other parts of New European Driving Cycle (NEDC) that they tested. Another engine operation mode that can produce significant amounts of secondary inorganic aerosol from gasoline vehicle exhaust is idling (Nordin et al., 2013).

Natural gas usage as a fuel in combustion engines, both in energy production and traffic, is a growing trend worldwide. Natural gas engines emit little primary particle mass and less CO_2 than engines fueled with conventional fuels (Anderson et al., 2015; Bielaczyc et al., 2014) but their particle number emission can be significant (Hallquist et al., 2013; Jayaratne et al., 2010). In addition, the size of the majority of the natural gas engine emitted particles can be below the detection limits of traditional exhaust particle measurement devices (Alanen et al., 2015). Natural gas engine exhaust particles are highly volatile (Bullock and Olfert, 2014; Jayaratne et al., 2012) or they can consist of volatile matter condensed on non-volatile cores (Alanen et al., 2015; Graves et al., 2015; Pirjola et al., 2016). The evaporation of the particles is largest at temperatures below 100 °C (Alanen et al., 2015; Jayaratne et al., 2012). Primary particles from natural gas engine mainly consist of organic matter (Pirjola et al., 2016) but the composition depends on exhaust after-treatment (Lehtoranta et al., 2016). In the study of Lehtoranta et al. (2016), high catalyst temperatures were found to increase the fraction of sulfate in particles when a combination of oxidative and reductive catalysts was employed. Also increased ammonium concentrations were found in particles at high catalyst temperatures.

To the authors' knowledge, there are no published studies on secondary particle formation from natural gas engine emission, its chemical or physical properties or the effect of exhaust after-treatment on exhaust's secondary particle formation. In this study, the secondary aerosol formation potential of natural gas engine exhaust was investigated by a flow-through reactor, and the chemical and physical characteristics of particles were investigated by aerosol instruments. The results were compared to the primary particle emission but because the primary particle emission of the same engine has already been discussed in two earlier publications (Alanen et al., 2015; Lehtoranta et al., 2016), it is not a focus of this paper. In general, this study aims to

Atmos. Chem. Phys. Discuss., doi:10.5194/acp-2017-44, 2017
Manuscript under review for journal Atmos. Chem. Phys.
Discussion started: 8 February 2017

Atmospheric Chemistry and Physics Discussions

report the total particulate emissions of natural gas engines, i.e. primary and secondary particles, to ensure that shifting into natural gas from diesel and gasoline does not cause unexpected environmental or health issues, and to define the possible benefits of the shift. Volatility studies on both primary and secondary particles enabled an evaluation of the stability and residence time of the particles in the atmosphere. The study of chemical composition can help solve their origin and find ways to reduce the particulate emission.

2 Methods

2.1 Engine and after-treatment

The engine used was a retrofitted spark ignition natural gas engine using Russian pipeline natural gas with methane content of 97 % and sulfur content below 1 ppm as fuel. The engine was run at two steady-state engine driving modes with torque 70 Nm and speed 2700 rpm (Mode 1, M1) and torque 35 Nm and speed 3100 rpm (Mode 2, M2). In the engine mode 2, short chain hydrocarbons were added into the exhaust in order to make it resemble the exhaust of a power plant NG engine. The retrofitting, natural gas and lubricating oil properties, and the engine driving modes have been described in more detail by Murtonen et al. (2016), Alanen et al. (2015) and Lehtoranta et al. (2016).

Two separate after-treatment systems were applied in the measurements, both consisting of a reductive and an oxidative section. The after-treatment has been described in more detail by Lehtoranta et al. (2016). The first catalyst (Catalyst 1, C1) consisted of only one reactor that targeted both the oxidation of carbon compounds and NO_x reduction with the use of urea injection in the same catalyst reactor. The second catalyst system (Catalyst 2, C2) consisted of a palladium and platinum containing methane oxidation catalyst followed by urea injection and a vanadium-SCR catalyst, which catalysts were supported on metallic honeycomb substrates. The catalyst 1 was used in three different exhaust temperatures in the range of 350-450 °C in order to study its performance and influence on secondary particle formation potential of the engine exhaust. The temperature of the catalyst 2 was 500 °C. The catalyst temperatures were measured upstream of the oxidation catalysts. The temperature prior to the SCR of catalyst 2 was approximately 50 °C lower than prior to the oxidation catalyst. The exhaust flow through the catalysts was kept constant 80 kg h^{-1} by leading only a part of the exhaust gas flow through them (Murtonen et al., 2016).

2.2 Instrumentation and data analysis

For the particle measurement instruments, the sampling system consisted of a porous tube diluter (PTD, Mikkanen and Moisio 2001; Ntziachristos et al. 2004) with dilution ratio (DR) 6, followed by an ejector diluter (Dekati Ltd.) with DR 4. The dilution ratio over the PTD was adjusted by a bypass flow mass flow controller placed downstream the residence time chamber (Fig. 1). The dilution ratios were calculated from CO_2 concentrations in raw and diluted exhaust sample and they could be used for calculations of tailpipe concentrations of particle emissions. The aerosol sampling was done downstream the exhaust after-treatment system.

Atmos. Chem. Phys. Discuss., doi:10.5194/acp-2017-44, 2017
Manuscript under review for journal Atmos. Chem. Phys.
Discussion started: 8 February 2017

Atmospheric Chemistry and Physics Discussions

A potential aerosol mass chamber (PAM, Kang et al., 2007, 2011; Lambe et al., 2011, 2015) was used to simulate the aging process of an aerosol in the atmosphere. In the PAM, an oxidative environment (O_3, OH and HO_2, UV-light) was produced by two UV lamps emitting 185 nm and 254 nm radiation in a small (13 l) flow-through chamber. The PAM chamber was placed between the two dilution stages and the flow through it was a constant 5 liters per minute (residence time 156 s), measured by a bubble flow meter (Gilibrator, Sensidyne Inc.) and adjusted by a pressure regulator of the compressed air flow to ejector diluter. The PAM chamber could be either bypassed or used in order to measure the properties of primary and secondary aerosols, respectively.

The approximate atmospheric age, i.e. photochemical age simulated by the PAM chamber UV-lights, was modeled using the properties of the PAM chamber and the measured concentrations of gaseous components that cause external OH reactivity in the chamber. The model used for calculating the OH exposures was based on the degradation mechanism extracted from the Master Chemical Mechanism, MCM v3.3.1, (Jenkin et al., 1997, 2003; Saunders et al., 2003) via website http://mcm.leeds.ac.uk/MCM and translated to Matlab code using the Kinetic PreProcessor, KPP (Damian et al., 2002).

MCM is a near-explicit chemical mechanism describing atmospheric degradation of volatile organic compounds in gas phase. MCM describes the degradation of a given VOC through different generations of products until ultimately CO_2 is formed. It contains about 17 000 reactions for 6 700 different species. (Jenkin et al., 1997, 2003; Saunders et al., 2003). To be able to use these mechanisms with the PAM chamber, the photolysis rates have been calculated for ultraviolet light with wavelengths of 185 nm and 254 nm. The absorption cross section and quantum yield values needed for this are IUPAC recommendations (Atkinson et al., 2007) supplemented with the JPL data evaluation number 18 (Burkholder et al., 2015) when necessary. Some photolysis reactions relevant to the PAM chamber, but missing from the tropospheric MCM schemes, have also been added.

KPP is a software tool for translating kinetic chemical mechanisms into Fortran77, Fortran90, C, or Matlab simulation code. The generated code produces concentrations of each species present as a function of time (Damian et al., 2002). For the model used, the KPP source code has been modified to fix certain conflicts with the MCM mechanism and the photolysis rate calculations written for the PAM chamber, as well as to allow large chemical schemes typical to MCM.

In this paper, we describe the PAM OH exposure as photochemical age which is the equivalent time in the atmosphere in which the sample would reach the same OH exposure as in the PAM chamber. Thus,

$$\text{Photochemical age (days)} = \frac{\text{OH exposure}}{1.5 * 10^6 \text{ molec. cm}^{-3}} \frac{1}{3600 \text{ h}^{-1}\text{s} * 24 \text{ d}^{-1}\text{h}}, \quad (1)$$

where $1.5 * 10^6$ molec. cm^{-3} is the average OH concentration in the atmosphere (Mao et al., 2009).

Relative humidity (RH) was measured downstream the PAM chamber. The RH was high, about 80 % due to the low primary dilution ratio that was applied during the experiments. The high RH of the sample complicated the evaluation of the PAM background mass levels, i.e. the particulate mass that was generated by only compressed air and UV lights, because the high RH could not be reproduced in the compressed air by the available instrumentation. The background levels were measured using both dry compressed air and compressed air with RH ~30 %.

Atmos. Chem. Phys. Discuss., doi:10.5194/acp-2017-44, 2017
Manuscript under review for journal Atmos. Chem. Phys.
Discussion started: 8 February 2017

Atmospheric Chemistry and Physics Discussions

NO_x concentration was measured by a chemiluminescence detector (CLD), CO and CO_2 concentrations in raw exhaust by a non-dispersive infrared (NDIR) analyzer and CO_2 concentration in diluted exhaust by a Sick Maihak SIDOR gas analyzer. Water, methane, NH_3, HNCO and the ratio of NO and NO_2 were measured by a Fourier transform infrared spectroscopy (FTIR, Gasmet Cr-2000) analyzer and methane, ethane, propane and ethylene were measured by a gas chromatograph (GC). Aerosol instruments covered a large particle mobility and aerodynamic size range and measurements of chemical composition of the particles. For the measurements of particle number, mass and size, an engine exhaust particle sizer (EEPS, TSI Inc., Mirme 1994) and a high-resolution low-pressure impactor (HRLPI, Arffman et al. 2014) were employed, both on one-second time resolution. EEPS measures the size distribution and concentration of particles with a mobility diameter of 5.6-560 nm and HRLPI the aerodynamic size distribution of particles ~5-200 nm. With an assumption of unit density and spherical particles, the mass of particles was calculated. EEPS default inversion was applied.

A soot particle aerosol mass spectrometer (SP-AMS, Aerodyne Research Inc., US), a combination of a high resolution time-of flight aerosol mass spectrometer and a single particle soot photometer (Droplet Measurement Technologies) measured the chemical composition and oxidative state of the aerosol sample. The SP-AMS measures both refractory and non-refractory particulate matter. It operated in V-mode, with one-minute time resolution measuring half of the time in mass spectra (MS) mode and the other half in particle size (pToF) mode. Both laser and tungsten vaporizers were used. The collection efficiency applied in the calculations was 0.5.

Volatility measurements were made with a thermodenuder described in the publication by Heikkilä et al. (2009). When the remaining mass of particles was measured in function of TD temperature, the thermodenuder was heated up to 265 °C and then switched off, the sample flow still flowing through it. The decreasing temperature was recorded for at least half an hour until the temperature was below 50 °C. Emission factors were calculated from engine performance information. Residual O_2 in exhaust was 6.2-6.3 %, the power of the engine was 12 kW and 20 kW and the combustion air flow into the engine were approximately 100 and 115 kg h^{-1} at the engine modes 1 and 2, respectively.

3 Results and discussion

3.1 Secondary particle formation and chemical composition

The concept “total aged” here comprises all particle mass measured downstream of the PAM chamber, i.e. both primary and secondary particle mass. In general, primary particle mass has not been subtracted from the mass measured downstream of the PAM (Total aged) to calculate secondary particle mass separately because it would have created inconsistency in representation of the results since e.g. particle size distributions or volatility behavior cannot be presented this way. For the same reasons, the PAM background mass, i.e. the particle mass generated in the PAM chamber from clean compressed air has not been subtracted, but presented separately in the supplementary section of this paper.

Figure 2 contains particulate mass measurement results derived from the three aerosol instruments. The chemical compositions from SP-AMS are also presented. The cases (engine mode, catalyst, catalyst temperature) included in this paper have been selected to be representative and have data collected with all available instruments at both primary and total aged aerosol

Atmos. Chem. Phys. Discuss., doi:10.5194/acp-2017-44, 2017
Manuscript under review for journal Atmos. Chem. Phys.
Discussion started: 8 February 2017

Atmospheric Chemistry and Physics Discussions

measurements. In most cases in our measurements, primary exhaust particle mass concentrations from the natural gas engine were close to the detection limits of instruments EEPS, HRLPI and SP-AMS (Alanen et al., 2015; Lehtoranta et al., 2016). Exceptions were made by high temperature catalyst cases (M2, C2, 500 °C and M2, C1, 450 °C) where more primary particle mass formed especially on the size ranges of the HRLPI and EEPS: a high catalyst temperature favors conversion of SO_2 into SO_3 and further into sulfuric acid that can nucleate and condensate on existing particles in the sampling process or when released into the atmosphere (see e.g. Arnold et al., 2012; Rönkkö et al., 2013). The primary particle formation phenomena and concentrations have been discussed in more detail in Lehtoranta et al. (2016) while this paper focuses on secondary aerosol formation and the total aged particle emission.

The formed secondary particle mass concentrations were found to be on a significantly high level in comparison with the primary particle mass emission. In all the investigated cases, particle mass increased when the sample was led through the PAM chamber. The increase in mass could be magnitudes larger than the primary particle mass emission (Table 1). The relative increase in mass in the PAM chamber could not be specified for all the HRLPI measurements because of the very low primary particle mass. Total aged aerosol mass produced by natural gas engine exhaust was 0.89-2.3 mg m^{-3} according to SP-AMS, leading to secondary mass production of 0.86-2.29 mg m^{-3}.

The secondary aerosol formation, i.e. the ratio of the total aged particulate mass and the primary particulate mass, was lower in the cases that already produced more primary particle mass, i.e. in the cases with a high catalyst temperature. It is possible that the particulate matter that would otherwise condense on particles in PAM chamber, or later on in the atmosphere when real-world emission is in question, condenses on particle phase already in the cooling and dilution process if the catalyst conditions are favorable. I.e. if the catalyst oxidizes the gases thus lowering their saturation vapor pressure and allowing them to condense or nucleate already when released into the atmosphere. A high catalyst temperature promoted larger total aged aerosol formation according to EEPS and HRLPI measurements. However, the SP-AMS total aged mass concentrations did not increase with an increasing catalyst temperature. The differences of instrument showing are discussed in Sect. 3.3.

The total aged aerosol of the natural gas engine exhaust consisted of both organic and inorganic matter at the tested operating conditions (Fig. 2, Table 1). Approximately half of the total aged aerosol particle mass detected by SP-AMS consisted of organic matter. The fraction of sulfate and nitrate was measured to be 34-49 % in total, their ratio depending on the case, and the fraction of ammonium varied between 10-15 %.

The organic fraction of the total aged aerosol consisted of hydrocarbon fragments (C_xH_y), fragments with one oxygen atom (C_xH_yO) and fragments with more than one oxygen atom ($C_xH_yO_{z,z>1}$); there was little or no C_xH_yN fragments (hydrocarbons with nitrogen) in the total aged particles. The main secondary organic ions detected by the SP-AMS were CO_2^+, CHO^+ and $C_2H_3O^+$. The composition of organic aerosol was similar in all the cases: $C_xH_yO_{z,z>1}$ group was the largest, followed by C_xH_y and C_xH_yO. The source of the secondary organic aerosol could be either the natural gas or the lubricating oil. We, however, are not able to tell the source based on these measurements.

O/C ratios of total aged aerosol measured by SP-AMS were between 0.9-1.2. The O/C ratio of the primary aerosol in the case with the largest concentration was slightly smaller (1.1) than the O/C ratio of the total aged aerosol in the same case (M2, C2, 500 °C). In all the other primary aerosol measurements the particle mass concentrations in the sample were too low for

Atmos. Chem. Phys. Discuss., doi:10.5194/acp-2017-44, 2017
Manuscript under review for journal Atmos. Chem. Phys.
Discussion started: 8 February 2017

Atmospheric Chemistry and Physics Discussions

O/C ratio analysis. In comparison with a secondary aerosol emission study for gasoline engines by Karjalainen et al. (2016), the observed O/C ratios in total aged aerosol from PAM chamber were rather high.

The simulated atmospheric, or photochemical, ages in the investigated cases varied between 4.6-10.7 days, depending on the external OH reactivity that was affected by the concentrations of gaseous emissions (Table 1) entering the PAM chamber and by the relative humidity of the sample. In the study of Tkacik et al. (2014), the peak secondary aerosol production took place after 1-1.5 days of equivalent atmospheric oxidation ([OH]=1.5*10^6 molec. cm^{-3}) when a vehicle fleet emissions in a highway tunnel was studied, and larger OH exposures started to reduce the secondary mass. In our study, the largest total aged particle concentrations were achieved with the longest atmospheric ages that were simulated by the PAM chamber and the lowest with the shortest atmospheric ages. However, the secondary aerosol formation potential can have been affected also by the engine parameters, not only the achieved photochemical age: the total aged particle concentrations were the highest on the engine operation mode 2 (M2). The variation in the atmospheric ages increases uncertainty in the case to case comparison of the gained results of secondary aerosol formation potential.

Emission factors or secondary aerosol production factors in different units can be calculated from the presented particle mass concentrations with use of following factors. If a unit factor mg kg_{fuel}^{-1} is needed a factor 20.6 m^3 kg_{fuel}^{-1} can be applied to multiply the particle concentration. In order to obtain emission and production factors in unit kWh^{-1}, a factor 2.7 m^3 kWh^{-1} (Mode 1) or 4 m^3 kWh^{-1} (Mode 2) can be similarly used. These factors are derived from the engine performance information provided in Sect. 2.2.

The production factors of secondary organic aerosol have been calculated and collected in Table 2 in unit kg_{fuel}^{-1}. To be able to compare the SOA production factors, here primary organic aerosol has been subtracted from the total aged organic aerosol. Table 2 contains also SOA production factors of secondary organic aerosol for different diesel and gasoline vehicles obtained from the literature. Although the total aged particulate matter production of the investigated NG engine was much larger than its primary particle emissions, they were smaller or on the similar level with SOA production both from diesel and gasoline engines in the literature. For example, the SOA formation potential from the NG engine, measured by SP-AMS, was similar to that from a diesel vehicle equipped with a catalytic converter or to that from a hot start gasoline vehicle. On the other hand, the photochemical age that was simulated by a chamber in the different studies, varied a lot. This is why the comparison of the SOA production factors should be done carefully. The longest atmospheric ages in the literature in Table 2 were achieved in our study.

3.2 Volatility of primary and secondary particle mass

The volatility of the particles was studied with a thermodenuder. Mass fraction remaining (MFR) stands for the fraction of the particle mass at a given thermodenuder temperature and the particle mass at room temperature. In Fig. 3, particle mass fraction remaining has been calculated for two representative cases of primary emission and four representative cases of total aged particle emission, selected amongst the cases already introduced. Figure 3 shows data only from EEPS since the curves obtained from HRLPI were similar. Here, the curves have been smoothed by a moving average but the original one-second-resolution figure can be found in the supplementary section. For the total aged emission, the cases with both higher and lower

Atmos. Chem. Phys. Discuss., doi:10.5194/acp-2017-44, 2017
Manuscript under review for journal Atmos. Chem. Phys.
Discussion started: 8 February 2017

Atmospheric Chemistry and Physics Discussions

catalyst temperature are presented. For primary particle emission only the case with higher catalyst temperature is presented. This is because an accurate examination of the volatility of primary particles on low catalyst temperatures cannot have been done due to the too low primary particle mass concentrations for high-quality analysis. In the figure, the "starting point", i.e. the temperature where the mass fraction remaining is one, is 50 °C and not lower because of the decelerated cooling of the thermodenuder towards the room temperature and related time limitations.

The MFR curves for each type of particles are characteristic, i.e. each particle type can easily be distinguished by their evaporation behavior. To highlight this, primary particle evaporation is marked with black, and total aged particle evaporation curves are marked with cyan and blue in Fig. 3. The volatility of particles from the natural gas engine clearly changes when the particles are aged. At high catalyst temperature, primary particles (black triangles in Fig. 3) are more volatile than the total aged particles (cyan squares). Approximately half (46-60 % in EEPS, 43-53 % in HRLPI) of the total aged particle mass remained at thermodenuder temperature 250 °C whereas only 5-10 % (1-4 % in HRLPI) of the primary particle mass remained at that temperature.

Also the catalyst temperature had an impact on the volatility of the total aged particles (blue vs. cyan). There was an easily evaporable fraction of the total aged particles that were formed in the case of a low catalyst temperature. The easily evaporable fraction evaporated below 110 °C. Because of this easily evaporable fraction, the MFR of total aged particles at 250 °C was 30 % in the low catalyst temperature cases while in the high catalyst temperature cases the MFR of total aged particles at 250 °C was 46-60 %.

The thermodenuder used in this study has been designed to minimize nanoparticle losses by reducing the residence time (Heikkilä et al., 2009). For example, in this study, the residence time in the heated zone of the thermodenuder was less than one second. An et al. (2007) measured oxidated α-pinene particles and observed that only half of the secondary particle mass evaporates in a thermodenuder (100 °C) if the residence times in the heated zone of the thermodenuder are less than a few seconds. With a longer residence times the remaining mass downstream the thermodenuder decreases to less than three percent. This means that the remaining fraction of particle mass in our study could have been smaller with longer residence times in the thermodenuder. On the other hand, a longer residence time in the thermodenuder would have increased the nanoparticle losses. In this study, with the use of a thermodenuder, we could observe the volatility differences between the different types of particle emissions emitted by a natural gas engine.

In Fig. 4 the remaining mass fractions are plotted for different chemical species of the particles drawn from the SP-AMS. In the primary emission case, approximately one third of particle mass, consisting mainly of organics, remained at TD temperature 250 °C. The low concentrations and particle size below the detection limit of SP-AMS degrades the analysis in the case M2, C1, 450 °C, seen as a fluctuating signal. In high catalyst temperature cases about 25 % of the total aged particle mass and in low catalyst temperature cases less than 10 % of total aged particle mass remained at 250 °C according to SP-AMS. The remaining particle matter consisted of organics, sulfate and ammonium, in this order.

Composition information reveals that the high-volatility fraction of the total aged particles in low temperature catalyst cases consisted of nitrates, possibly of ammonium nitrate, and high-volatility organics. Primary particle sulfate evaporated at thermodenuder temperatures between 100-170 °C and the total aged particle sulfate above 160 °C. In all types of particles, the

Atmos. Chem. Phys. Discuss., doi:10.5194/acp-2017-44, 2017
Manuscript under review for journal Atmos. Chem. Phys.
Discussion started: 8 February 2017

Atmospheric Chemistry and Physics Discussions

evaporation of organics was steady and gradual below 200 °C, indicating various organic compounds with different evaporation temperatures. Above 200 °C the evaporation of organics decreased. This combined SP-AMS and EEPS/HRLPI derived thermodenuder temperature ramp information can be used in future measurements for particle composition analysis: the evaporation temperature of the particles can give valuable information of the composition of the particles also without an access to SP-AMS.

The temperatures where 50 % of the volatile fraction of the chemical compounds of the particles are remaining are collected in Table 3. The case "Primary, M2, C1, 450 °C" had too low particle mass concentrations (See Fig. 4) for this kind of examination. The evaporation temperature of sulfate and nitrate were the highest and the lowest, respectively, in all analyzed cases (all catalyst temperatures, primary and total aged particles). Similarly to Huffman et al. (2009) who measured ambient aerosol volatility in megacities with a thermodenuder and an SP-AMS, we found that nitrate has the highest volatility and sulfate the lowest.

Robinson et al. (2007) and Huffman et al. (2009) propose that all organic aerosol should be considered as semivolatile. Our results on primary and PAM chamber generated organic aerosols point to that direction as well. The evaporation temperature of the volatile fraction ($T_{volatile,\ 50\ \%}$) of organic matter lay between the $T_{volatile,\ 50\ \%}$ of nitrate and sulfate in all cases. Also, a significant fraction of the mass concentration of the organic matter did not evaporate. More exact specification of the volatility cannot be given but there is room left for speculation if a part of the organic matter in secondary particles is SV-SOA or LV-SOA (Murphy et al., 2014).

The evaporation of ammonium in total aged particles took place at higher thermodenuder temperatures when the catalyst temperature was high. The theory that the sulfate-nitrate trade-off phenomenon that determines the formation of nitrates is ammonium-bound is supported by the evaporation temperatures of ammonium. Ammonium was evaporated at over 50 °C higher thermodenuder temperatures in the high catalyst temperature cases (Table 3), thus its evaporation temperature was closer to the evaporation temperature of sulfate when the sulfate concentration of the particles was larger. By contrast, in the low catalyst temperature cases where the nitrate concentration was higher, the evaporation temperature of ammonium was closer to that of nitrate.

The nitrate concentrations that were measured during the thermodenuder temperature ramp (Fig. 4) in low thermodenuder temperatures differ from the nitrate concentrations that were measured without a thermodenuder (Fig. 2 a+b) in total aged particles. A possible explanation is a long time needed for the stabilization of the nitrate concentration. In our measurement protocol, 10-15 minutes was waited after switching the PAM UV-lights on, followed by a 10-minute steady-state measurement with the aerosol instruments. After this a thermodenuder ramp, that took approximately 45 minutes, was started. Based on the results, the 10-15-minute wait was insufficient if accurate nitrate concentrations were desired. Therefore, the chemical compound measurements performed on low thermodenuder temperature can give a truer picture of the secondary aerosol formation than the measurements presented in Fig. 2. The change in concentrations between the steady-state measurements and the thermodenuder ramp measurements is the largest for nitrate but also the concentrations of other compounds slightly differ from each other. Because the nitrate concentrations were found to be the slowest to stabilize and the most sensitive on

Atmos. Chem. Phys. Discuss., doi:10.5194/acp-2017-44, 2017
Manuscript under review for journal Atmos. Chem. Phys.
Discussion started: 8 February 2017

Atmospheric Chemistry and Physics Discussions

changes in the system, such as temperature, special attention should be paid on measurements of nitrate, especially when a PAM chamber is being used.

According to our thermodenuder temperature ramp experiments, the catalyst temperature affected total aged particle composition. With a decreasing catalyst temperature, the mass concentration and fraction of sulfate in total aged particles decreased (Fig. 4). This was expected; at lower catalyst temperatures the oxidation of SO_2 to SO_3 decreases and less sulfuric acid (sulfates) can form (Arnold et al., 2012). The mass fraction of nitrate in secondary particles increased with a decreasing catalyst temperature. This could not be explained by catalyst performance improvement: gaseous NO_x levels remained similar in all catalyst temperatures or rose with an increasing catalyst temperature (see Lehtoranta et al., 2016). Sulfate concentrations, however, could explain the behavior of nitrate concentrations: If enough gaseous sulfuric acid is available, ammonium sulfate forms, and if not, more ammonium nitrate can form instead. Similar behavior of nitrate and sulfate trade-off has been measured by Ntziachristos et al. (2016) for two different marine fuels, namely heavy fuel oil (HFO) and light fuel oil (LFO).

3.3 Differences between instruments and mass size distributions

Slightly unexpectedly, the total aged particle mass measured by SP-AMS was 2-4 times larger than the total mass measured by EEPS and 1-3 times larger than that measured by HRLPI (Fig. 2). There could be several reasons for that. In EEPS and HRLPI, unit density and spherical particles have been assumed in the mass calculations. Natural gas engine primary particles have density 0.85 g cm^{-3} (Bullock and Olfert, 2014) but the densities of natural gas engine secondary particles can be larger than unit density. For example, the density of ammonium nitrate, ammonium sulfate and sulfuric acid are approximately 1.5, 1.5 and 1.8 g m^{-3}, respectively (Clegg and Wexler, 2011). Particle density does not explain the difference in instrument readings totally. Also the collection efficiency (CE) estimation used in SP-AMS calculation is probably not the reason for differences between instrument results in this study. Evaluation of the CE following the procedure of Middlebrook et al. (2012) reveals that CE = 0.5 is a good estimation for the studied total aged particles.

However, detection efficiency and size range vary between the aerosol instruments (EEPS 5.6-560 nm, HRLPI ~5-200 nm, SP-AMS ~30-1000 nm) and can explain the differences in results; HRLPI can detect a larger fraction of the primary particles than SP-AMS because of the more suitable size range of the instrument and, correspondingly, SP-AMS can detect a larger fraction of the total aged particles formed in PAM chamber because of its more suitable size range.

In Fig. 5, mass size distributions of EEPS and HRLPI are plotted. HRLPI suggests a part of the particle mass to lie above the instrument size range, which is confirmed by SP-AMS mass size distributions in Fig. 6. According to SP-AMS mass size distributions of total aged particles are bimodal, the size of the larger mode being at 480-840 nm and the smaller at 150-200 nm. However, although the mass concentration of the total aged particles is better recorded by SP-AMS, a part of the particles on the smallest particle sizes is missed due to the lower limit of SP-AMS size range at 30-50 nm.

We can also see a difference between EEPS and HRLPI mass size distributions. The difference is probably due to the inversion of EEPS that forces the size distributions to follow log-normal shape. The different measurement principle of the instruments must also be kept in mind. EEPS measures the mobility size and HRLPI the aerodynamic size of the particles.

Atmos. Chem. Phys. Discuss., doi:10.5194/acp-2017-44, 2017
Manuscript under review for journal Atmos. Chem. Phys.
Discussion started: 8 February 2017

Atmospheric Chemistry and Physics Discussions

4 Conclusions

Natural gas engines emit very little particle mass which can make them less harmful on human health than gasoline or diesel fueled engines. However, also secondary aerosol formation increases human exposure to aerosol particles. When natural gas engines become more common in traffic and energy production, also their secondary particle formation potential becomes more important and an even more relevant object for research. Therefore, the potential reduction of the total aerosol particle mass and related health and climate effects when shifted from liquid fuels to natural gas or biogas in combustion engines is important.

In this study, a retro-fitted natural gas engine equipped with exhaust after-treatment was studied in laboratory in an engine test bench, using steady-state engine operation modes i.e., constant engine speed and torque. The secondary aerosol formation was studied using a potential aerosol mass (PAM) chamber. Estimates for the atmospheric ages achieved by the PAM chamber were 4.6-10.7 days. In this study, secondary aerosol mass potential of natural gas emission was measured to be on a small or medium level, but well measurable. Compared to the primary particle mass emissions of the same engine, the secondary aerosol formation potential was substantial: approximately one to two orders of magnitude higher than the primary aerosol mass. However, the very small primary particle masses in some of the observed engine and catalyst operation modes complicated this kind of comparison. In comparison with diesel and gasoline fueled vehicles, the secondary organic aerosol formation potential was small or moderate, depending on the fuel and the exhaust after-treatment of the reference. The SOA formation potential was on the same level or lower than the SOA formation potential of a diesel vehicle equipped with an oxidation catalyst or that of warm (hot start) gasoline vehicles. However, the photochemical age that was produced by the PAM chamber in our study was longer than the photochemical ages achieved in the previous studies. In our study, the largest SOA mass was produced with the longest photochemical ages.

The total aged aerosol, i.e. combined primary and secondary aerosol (downstream of a PAM chamber) of the NG engine consisted of organic matter, nitrate, sulfate and ammonium, roughly in this order. It was found that aging of the exhaust generates low-volatility organics. However, the composition of the secondary aerosol was for the most part inorganic; the fraction of organic matter in the secondary particles varied between 37-56 %.

Exhaust after-treatment was found to have an effect on the secondary aerosol composition. High catalyst temperature promoted the formation of sulfate particles in total aged aerosol, whereas low catalyst temperature promoted nitrate formation. Because the quantity NO_x emission was reduced at the lower catalyst temperatures, it was concluded that the formation of nitrate in particles (total aged) depended on the sulfate particle formation rather than the NO_x emission. Sulfate and nitrate are likely to exist in the forms of ammonium sulfate and ammonium nitrate. Therefore, what limits the nitrate mass in particles is most likely the availability of ammonia. However, a more thorough research on the nitrate content in secondary aerosol is needed in order to confirm these findings.

The total aged nanoparticles formed from the natural gas exhaust were found to be less volatile than the primary particles. This can affect their lifetime in the atmosphere and therefore their impact on radiative balance of the atmosphere or their

potential to act as cloud nuclei. A higher catalyst temperature impacts the total aged particles by decreasing their volatility, or, by decreasing their volatile fraction.

In our study, only one constant PAM UV-light voltage could be used. With an improved instrumentation, a broader variation in light intensity could be achieved, thus improving our knowledge in the evolution of the secondary aerosol and providing a better understanding especially on the SOA production potential differences in different catalyst conditions. Also, because natural gas is not the only widely used gaseous fuel, the secondary aerosol formation potential of a more extensive fuel selection would be interesting to study. The role of lubricating oil is also not known yet – studies performed at different natural gas combustion sites and with various lubricating oils would reveal its significance to secondary aerosol formation.

5 Data and code availability

The data and code of this study are available from the authors upon request.

Competing interests.

The authors declare that they have no conflict of interest.

Acknowledgements. This study was funded by Tekes, the Finnish Funding Agency for Innovation, Neste, AGCO Power, Wärtsilä, Dinex Ecocat, Dekati, Suomi Analytics and Viking Line. Jenni Alanen acknowledges Gasum gas funding for financial support. Pauli Simonen acknowledges TUT Graduate School for funding. Oskari Kangasniemi acknowledges Nessling Foundation for funding. Topi Rönkkö acknowledges the financial support from the Academy of Finland (ELTRAN project, grant number 293437).

Atmos. Chem. Phys. Discuss., doi:10.5194/acp-2017-44, 2017
Manuscript under review for journal Atmos. Chem. Phys.
Discussion started: 8 February 2017

Atmospheric Chemistry and Physics Discussions

References

Alanen, J., Saukko, E., Lehtoranta, K., Murtonen, T., Timonen, H., Hillamo, R., Karjalainen, P., Kuuluvainen, H., Harra, J., Keskinen, J., and Rönkkö, T.: The formation and physical properties of the particle emissions from a natural gas engine, Fuel, 162, 155–161, doi:10.1016/j.fuel.2015.09.003, 2015.

An, W. J., Pathak, R. K., Lee, B. H., and Pandis, S. N.: Aerosol volatility measurement using an improved thermodenuder: Application to secondary organic aerosol, Journal of Aerosol Science, 38, 305–314, doi:10.1016/j.jaerosci.2006.12.002, 2007.

Anderson, M., Salo, K., and Fridell, E.: Particle- and Gaseous Emissions from an LNG Powered Ship, Environmental Science and Technology, 49, 12 568–12 575, doi:10.1021/acs.est.5b02678, 2015.

Arffman, A., Yli-Ojanperä, J., Kalliokoski, J., Harra, J., Pirjola, L., Karjalainen, P., Rönkkö, T., and Keskinen, J.: High-resolution low-pressure cascade impactor, Journal of Aerosol Science, 78, 97–109, doi:10.1016/j.jaerosci.2014.08.006, 2014.

Arnold, F., Pirjola, L., Rönkkö, T., Reichl, U., Schlager, H., Lähde, T., Heikkilä, J., and Keskinen, J.: First online measurements of sulfuric acid gas in modern heavy-duty diesel engine exhaust: Implications for nanoparticle formation, Environmental Science and Technology, 46, 11 227–11 234, doi:10.1021/es302432s, 2012.

Atkinson, R., Baulch, D., Cox, R., Crowley, J., Hampson, R., Hynes, R., Jenkin, M., Kerr, J., Rossi, M., and Troe, J.: "IUPAC Subcommittee for gas kinetic data evaluation", Evaluated kinetic data:, http://www.iupac-kinetic.ch.cam.ac.uk, 2007.

Bahreini, R., Middlebrook, A. M., Brock, C. A., Gouw, J. A. D., Mckeen, S. A., Williams, L. R., Daumit, K. E., Lambe, A. T., Massoli, P., Canagaratna, M. R., Ahmadov, R., Carrasquillo, A. J., Cross, E. S., Ervens, B., Holloway, J. S., Hunter, J. F., Onasch, T. B., Pollack, I. B., Roberts, J. M., Ryerson, T. B., Warneke, C., Davidovits, P., Worsnop, D. R., and Kroll, J. H.: Mass Spectral Analysis of Organic Aerosol Formed Downwind of the Deepwater Horizon Oil Spill : Field Studies and Laboratory Confirmations, Environmental Science & Technology, 46, 8025–8034, doi:10.1126/science.1200320, 2012.

Bielaczyc, P., Woodburn, J., and Szczotka, A.: An assessment of regulated emissions and CO2 emissions from a European light-duty CNG-fueled vehicle in the context of Euro 6 emissions regulations, Applied Energy, 117, 134–141, doi:10.1016/j.apenergy.2013.12.003, 2014.

Bullock, D. S. and Olfert, J. S.: Size, volatility, and effective density of particulate emissions from a homogeneous charge compression ignition engine using compressed natural gas, Journal of Aerosol Science, 75, 1–8, doi:10.1016/j.jaerosci.2014.04.005, 2014.

Burkholder, J. B., Sander, S. P., Abbatt, J., Barker, J. R., Huie, R. E., Kolb, C. E., Kurylo, M. J., Orkin, V. L., Wilmouth, D. M., and H., W. P.: "Chemical Kinetics and Photochemical Data for Use in Atmospheric Studies, Evaluation No. 18," JPL Publication 15-10, Jet Propulsion Laboratory, Pasadena, http://jpldataeval.jpl.nasa.gov, 2015.

Chirico, R., Decarlo, P. F., Heringa, M. F., Tritscher, T., Richter, R., Prévôt, A. S. H., Dommen, J., Weingartner, E., Wehrle, G., Gysel, M., Laborde, M., and Baltensperger, U.: Impact of aftertreatment devices on primary emissions and secondary organic aerosol formation potential from in-use diesel vehicles: Results from smog chamber experiments, Atmospheric Chemistry and Physics, 10, 11 545–11 563, doi:10.5194/acp-10-11545-2010, 2010.

Clegg, S. L. and Wexler, A. S.: Densities and Apparent Molar Volumes of Atmospherically Important Electrolyte Solutions . 2 . The Systems H^+ - HSO_4^- - SO_4^{2-} - H_2O from 0 to 3 mol kg^{-1} as a Function of Temperature and a Pitzer Ion Interaction Model, and $(NH_4)_3H(SO_4)_2$ - H_2O and over Entire Concentration Range, The Journal of Physical Chemistry A, 115, 3461–3474, doi:10.1021/jp1089933, 2011.

Damian, V., Sandu, A., Damian, M., Potra, F., and Carmichael, G. R.: The kinetic preprocessor KPP-a software environment for solving chemical kinetics, Computers & Chemical Engineering, 26, 1567–1579, doi:10.1016/S0098-1354(02)00128-X, 2002.

Dockery, D. and Pope III, A.: Acute Respiratory Effects of Particulate Air Pollution., Annual Review of Public Health, 15, 107–132, 1994.

Gordon, T. D., Tkacik, D. S., Presto, A. A., Zhang, M., Jathar, S. H., Nguyen, N. T., Massetti, J., Truong, T., Cicero-Fernandez, P., Maddox, C., Rieger, P., Chattopadhyay, S., Maldonado, H., Maricq, M. M., and Robinson, A. L.: Primary gas- and particle-phase emissions and secondary organic aerosol production from gasoline and diesel off-road engines, Environmental Science and Technology, 47, 14 137–14 146, doi:10.1021/es403556e, 2013.

Gordon, T. D., Presto, A. A., May, A. A., Nguyen, N. T., Lipsky, E. M., Donahue, N. M., Gutierrez, A., Zhang, M., Maddox, C., Rieger, P., Chattopadhyay, S., Maldonado, H., Maricq, M. M., and Robinson, A. L.: Secondary organic aerosol formation exceeds primary particulate matter emissions for light-duty gasoline vehicles, Atmospheric Chemistry and Physics, 14, 4661–4678, doi:10.5194/acp-14-4661-2014, 2014a.

Gordon, T. D., Presto, A. A., Nguyen, N. T., Robertson, W. H., Na, K., Sahay, K. N., Zhang, M., Maddox, C., Rieger, P., Chattopadhyay, S., Maldonado, H., Maricq, M. M., and Robinson, A. L.: Secondary organic aerosol production from diesel vehicle exhaust: Impact of aftertreatment, fuel chemistry and driving cycle, Atmospheric Chemistry and Physics, 14, 4643–4659, doi:10.5194/acp-14-4643-2014, 2014b.

Graves, B., Olfert, J., Patychuk, B., Dastanpour, R., and Rogak, S.: Characterization of Particulate Matter Morphology and Volatility from a Compression-Ignition Natural-Gas Direct-Injection Engine, Aerosol Science and Technology, 49, 589–598, doi:10.1080/02786826.2015.1050482, 2015.

Hallquist, Å. M., Jerksjö, M., Fallgren, H., Westerlund, J., and Sjödin, Å.: Particle and gaseous emissions from individual diesel and CNG buses, Atmospheric Chemistry and Physics, 13, 5337–5350, doi:10.5194/acp-13-5337-2013, 2013.

Hallquist, M., Wenger, J. C., Baltensperger, U., Rudich, Y., Simpson, D., Claeys, M., Dommen, J., Donahue, N. M., George, C., Goldstein, A. H., Hamilton, J. F., Herrmann, H., Hoffmann, T., Iinuma, Y., Jang, M., Jenkin, M., Jimenez, J. L., Kiendler-Scharr, A., Maenhaut, W., McFiggans, G., Mentel, T. F., Monod, A., Prevot, A. S. H., Seinfeld, J. H., Surratt, J. D., Szmigielski, R., and Wildt, J.: The formation, properties and impact of secondary organic aerosol: current and emerging issues, Atmospheric Chemistry and Physics Discussions, 9, 3555–3762, doi:10.5194/acpd-9-3555-2009, 2009.

Heikkilä, J., Rönkkö, T., Lähde, T., Lemmetty, M., Arffman, A., Virtanen, A., Keskinen, J., Pirjola, L., and Rothe, D.: Effect of open channel filter on particle emissions of modern diesel engine., Journal of the Air & Waste Management Association (1995), 59, 1148–1154, doi:10.3155/1047-3289.59.10.1148, 2009.

Huang, R. J., Zhang, Y., Bozzetti, C., Ho, K. F., Cao, J. J., Han, Y., Daellenbach, K. R., Slowik, J. G., Platt, S. M., Canonaco, F., Zotter, P., Wolf, R., Pieber, S. M., Bruns, E. A., Crippa, M., Ciarelli, G., Piazzalunga, A., Schwikowski, M., Abbaszade, G., Schnelle-Kreis, J., Zimmermann, R., An, Z., Szidat, S., Baltensperger, U., El Haddad, I., and Prevot, A. S.: High secondary aerosol contribution to particulate pollution during haze events in China, Nature, 514, 218–222, doi:10.1038/nature13774, 2014.

Huffman, J. A., Docherty, K. S., Aiken, A. C., Cubison, M. J., Ulbrich, I. M., DeCarlo, P. F., Sueper, D., Jayne, J. T., Worsnop, D. R., Ziemann, P. J., and Jimenez, J. L.: Chemically-resolved aerosol volatility measurements from two megacity field studies, Atmospheric Chemistry and Physics, 9, 7161–7182, doi:10.5194/acpd-9-2645-2009, 2009.

Jathar, S. H., Miracolo, M. A., Tkacik, D. S., Donahue, N. M., Adams, P. J., and Robinson, A. L.: Secondary organic aerosol formation from photo-oxidation of unburned fuel: Experimental results and implications for aerosol formation from combustion emissions, Environmental science & technology, 47, 12 886–12 893, 2013.

Jayaratne, E. R., Meyer, N. K., Ristovski, Z. D., Morawska, L., and Miljevic, B.: Critical Analysis of High Particle Number Emissions from Accelerating Compressed Natural Gas Buses, Environmental Science and Technology, 44, 3724–3731, 2010.

Jayaratne, E. R., Meyer, N. K., Ristovski, Z. D., and Morawska, L.: Volatile properties of particles emitted by compressed natural gas and diesel buses during steady-state and transient driving modes, Environmental Science and Technology, 46, 196–203, doi:10.1021/es2026856, 2012.

Jenkin, M. E., Saunders, S. M., and Pilling, M. J.: The tropospheric degradation of volatile organic compounds: A protocol for mechanism development, Atmospheric Environment, 31, 81–104, doi:10.1016/S1352-2310(96)00105-7, 1997.

Jenkin, M. E., Saunders, S. M., Wagner, V., and Pilling, M. J.: Protocol for the development of the Master Chemical Mechanism, MCM v3 (Part A): tropospheric degradation of non-aromatic volatile organic compounds, Atmospheric Chemistry and Physics, 3, 161–180, doi:10.5194/acp-3-161-2003, 2003.

Jimenez, J. L., Canagaratna, M. R., Donahue, N. M., Prevot, A. S. H., Zhang, Q., Kroll, J. H., Decarlo, P. F., Allan, J. D., Coe, H., Ng, N. L., Aiken, A. C., Ulbrich, I. M., Grieshop, A. P., Duplissy, J., Wilson, K. R., Lanz, V. A., Hueglin, C., Sun, Y. L., Tian, J., Laaksonen, A., Raatikainen, T., Rautiainen, J., Vaattovaara, P., Ehn, M., Kulmala, M., Tomlinson, J. M., Cubison, M. J., Dunlea, E. J., Alfarra, M. R., Williams, P. I., Bower, K., Kondo, Y., Schneider, J., Drewnick, F., Borrmann, S., Weimer, S., Demerjian, K., Salcedo, D., Cottrell, L., Takami, A., Miyoshi, T., Shimono, A., Sun, J. Y., Zhang, Y. M., Dzepina, K., Sueper, D., Jayne, J. T., Herndon, S. C., Williams, L. R., Wood, E. C., Middlebrook, A. M., Kolb, C. E., Baltensperger, U., and Worsnop, D. R.: Evolution of Organic Aerosols in the Atmosphere, Science, 326, 1525–1529, 2009.

Kanakidou, M., Seinfeld, J. H., Pandis, S. N., Barnes, I., Dentener, F. J., Facchini, M. C., Van Dingenen, R., Ervens, B., Nenes, A., Nielsen, C. J., Swietlicki, E., Putaud, J. P., Balkanski, Y., Fuzzi, S., Horth, J., Moortgat, G. K., Winterhalter, R., Myhre, C. E. L., Tsigaridis, K., Vignati, E., Stephanou, E. G., and Wilson, J.: Organic aerosol and global climate modelling: A review, Atmospheric Chemistry and Physics, 5, 1053–1123, 2005.

Kang, E., Root, M. J., and Brune, W. H.: Introducing the concept of Potential Aerosol Mass (PAM), Atmospheric Chemistry and Physics Discussions, 7, 9925–9972, doi:10.5194/acpd-7-9925-2007, 2007.

Kang, E., Toohey, D. W., and Brune, W. H.: Dependence of SOA oxidation on organic aerosol mass concentration and OH exposure: Experimental PAM chamber studies, Atmospheric Chemistry and Physics, 11, 1837–1852, doi:10.5194/acp-11-1837-2011, 2011.

Karjalainen, P., Timonen, H., Saukko, E., Kuuluvainen, H., Saarikoski, S., Aakko-Saksa, P., Murtonen, T., Dal Maso, M., Ahlberg, E., Svenningsson, B., Brune, W. H., Hillamo, R., Keskinen, J., and Rönkkö, T.: Time-resolved characterization of primary and secondary particle emissions of a modern gasoline passenger car, Atmospheric Chemistry and Physics, 16, 8559–8470, doi:10.5194/acp-16-8559-2016, 2016.

Künzi, L., Krapf, M., Daher, N., Dommen, J., Jeannet, N., Schneider, S., Platt, S., Slowik, J. G., Baumlin, N., Salathe, M., Prévôt, A. S. H., Kalberer, M., Strähl, C., Dümbgen, L., Sioutas, C., Baltensperger, U., and Geiser, M.: Toxicity of aged gasoline exhaust particles to normal and diseased airway epithelia, Scientific Reports, 5, 11 801, doi:10.1038/srep11801, 2015.

Lambe, A. T., Ahern, A. T., Williams, L. R., Slowik, J. G., Wong, J. P. S., Abbatt, J. P. D., Brune, W. H., Ng, N. L., Wright, J. P., Croasdale, D. R., Worsnop, D. R., Davidovits, P., and Onasch, T. B.: Characterization of aerosol photooxidation flow reactors: Heterogeneous oxidation, secondary organic aerosol formation and cloud condensation nuclei activity measurements, Atmospheric Measurement Techniques, 4, 445–461, doi:10.5194/amt-4-445-2011, 2011.

Lambe, A. T., Chhabra, P. S., Onasch, T. B., Brune, W. H., Hunter, J. F., Kroll, J. H., Cummings, M. J., Brogan, J. F., Parmar, Y., Worsnop, D. R., Kolb, C. E., and Davidovits, P.: Effect of oxidant concentration, exposure time, and seed particles on secondary organic aerosol chemical composition and yield, Atmospheric Chemistry and Physics, 15, 3063–3075, doi:10.5194/acp-15-3063-2015, 2015.

Lehtoranta, K., Murtonen, T., Vesala, H., Koponen, P., Alanen, J., Simonen, P., Rönkkö, T., Timonen, H., Saarikoski, S., Maunula, T., Kallinen, K., and Korhonen, S.: Natural gas engine emission reduction by catalysts, Submitted to Emission Control Science & Technology, 2016.

Lelieveld, J., Evans, J. S., Fnais, M., Giannadaki, D., and Pozzer, A.: The contribution of outdoor air pollution sources to premature mortality on a global scale., Nature, 525, 367–71, doi:10.1038/nature15371, 2015.

Mao, J., Ren, X., Brune, W. H., Olson, J. R., Crawford, J. H., Fried, A., Huey, L. G., Cohen, R. C., and Heikes, B.: Airborne measurement of OH reactivity during INTEX-B, Atmospheric Chemistry and Physics, 9, 163–173, 2009.

McWhinney, R. D., Gao, S. S., Zhou, S., and Abbatt, J. P. D.: Evaluation of the effects of ozone oxidation on redox-cycling activity of two-stroke engine exhaust particles, Environmental Science and Technology, 45, 2131–2136, doi:10.1021/es102874d, 2011.

Middlebrook, A. M., Bahreini, R., Jimenez, J. L., and Canagaratna, M. R.: Evaluation of Composition-Dependent Collection Efficiencies for the Aerodyne Aerosol Mass Spectrometer using Field Data, Aerosol Science and Technology, 46, 258–271, doi:10.1080/02786826.2011.620041, 2012.

Mikkanen, P. and Moisio, M.: Sampling Method for Particle Measurements of Vehicle Exhaust, SAE International Journal of Fuels and Lubricants, pp. 1–6, 2001.

Mirme, A.: Electrical aerosol spectrometry, Ph.D. thesis, University of Tartu, 1994.

Murphy, B. N., Donahue, N. M., Robinson, A. L., and Pandis, S. N.: A naming convention for atmospheric organic aerosol, Atmospheric Chemistry and Physics, 14, 5825–5839, doi:10.5194/acp-14-5825-2014, 2014.

Murtonen, T., Lehtoranta, K., Korhonen, S., and Vesala, H.: Imitating emission matrix of large natural catalyst studies in engine laboratory, CIMAC congress, 2016.

Myhre, G., Shindell, D., Bréon, F. M., Collins, W., Fuglestvedt, J., Huang, J., Koch, D., Lamarque, J. F., Lee, D., and Mendoza, B.: Anthropogenic and natural radiative forcing, Climate change, 423, 2013.

Nordin, E. Z., Eriksson, A. C., Roldin, P., Nilsson, P. T., Carlsson, J. E., Kajos, M. K., Hellén, H., Wittbom, C., Rissler, J., Löndahl, J., Swietlicki, E., Svenningsson, B., Bohgard, M., Kulmala, M., Hallquist, M., and Pagels, J. H.: Secondary organic aerosol formation from idling gasoline passenger vehicle emissions investigated in a smog chamber, Atmospheric Chemistry and Physics, 13, 6101–6116, doi:10.5194/acp-13-6101-2013, 2013.

Ntziachristos, L., Giechaskiel, B., Pistikopoulos, P., Samaras, Z., Mathis, U., Mohr, M., Ristimaki, J., Keskinen, J., Mikkanen, P., Casati, R., Scheer, V., and Vogt, R.: Performance evaluation of a novel sampling and measurement system for exhaust particle characterization, SAE 2004 World Congress and Exhibition, 2004-01-14, doi:10.4271/2004-01-1439, 2004.

Ntziachristos, L., Saukko, E., Rönkkö, T., Lehtoranta, K., Timonen, H., Hillamo, R., and Keskinen, J.: Impact of sampling conditions and procedure on particulate matter emissions from a marine diesel engine, CIMAC congress, 2016.

Pirjola, L., Dittrich, A., Niemi, J. V., Saarikoski, S., Timonen, H., Kuuluvainen, H., Järvinen, A., Kousa, A., Rönkkö, T., and Hillamo, R.: Physical and Chemical Characterization of Real-World Particle Number and Mass Emissions from City Buses in Finland, doi:10.1021/acs.est.5b04105, 2016.

Platt, S. M., El Haddad, I., Zardini, A. A., Clairotte, M., Astorga, C., Wolf, R., Slowik, J. G., Temime-Roussel, B., Marchand, N., Ježek, I., Drinovec, L., Mocnik, G., Möhler, O., Richter, R., Barmet, P., Bianchi, F., Baltensperger, U., and Prévôt, A. S. H.: Secondary organic aerosol formation from gasoline vehicle emissions in a new mobile environmental reaction chamber, Atmospheric Chemistry and Physics, 13, 9141–9158, doi:10.5194/acp-13-9141-2013, 2013.

Rager, J. E., Lichtveld, K., Ebersviller, S., Smeester, L., Jaspers, I., Sexton, K. G., and Fry, R. C.: A toxicogenomic comparison of primary and photochemically altered air pollutant mixtures, Environmental Health Perspectives, 119, 1583–1589, doi:10.1289/ehp.1003323, 2011.

Robinson, A. L., Donahue, N. M., Shrivastava, M. K., Weitkamp, E. A., Sage, A. M., Grieshop, A. P., Lane, T. E., Pierce, J. R., and Pandis, S. N.: Rethinking Organic Aerosols: Semivolatile Emissions and Photochemical Aging, Science, 315, 1259–1262, doi:10.1126/science.1133061, 2007.

Rönkkö, T., Lähde, T., Heikkilä, J., Pirjola, L., Bauschke, U., Arnold, F., Schlager, H., Rothe, D., Yli-Ojanperä, J., and Keskinen, J.: Effects of gaseous sulphuric acid on diesel exhaust nanoparticle formation and characteristics, Environmental Science and Technology, 47, 11 882–11 889, doi:10.1021/es402354y, 2013.

Samy, S. and Zielinska, B.: Secondary organic aerosol production from modern diesel engine emissions, Atmospheric Chemistry and Physics, 10, 609–625, 2010.

Saunders, S. M., Jenkin, M. E., Derwent, R. G., and Pilling, M. J.: Protocol for the development of the Master Chemical Mechanism, MCM v3 (Part A): tropospheric degradation of non-aromatic volatile organic compounds, Atmospheric Chemistry and Physics, 3, 161–180, doi:10.5194/acp-3-161-2003, 2003.

Tkacik, D. S., Lambe, A. T., Jathar, S., Li, X., Presto, A. A., Zhao, Y., Blake, D., Meinardi, S., Jayne, J. T., Croteau, P. L., and Robinson, A. L.: Secondary organic aerosol formation from in-use motor vehicle emissions using a potential aerosol mass reactor, Environmental Science and Technology, 48, 11 235–11 242, doi:10.1021/es502239v, 2014.

Virtanen, A., Joutsensaari, J., Koop, T., Kannosto, J., Yli-Pirilä, P., Leskinen, J., Mäkelä, J. M., Holopainen, J. K., Pöschl, U., Kulmala, M., Worsnop, D. R., and Laaksonen, A.: An amorphous solid state of biogenic secondary organic aerosol particles. SI, Nature, 467, 824–7, doi:10.1038/nature09455, 2010.

Weitkamp, E. A., Sage, A. M., Pierce, J. R., Donahue, N. M., and Robinson, A. L.: Organic aerosol formation from photochemical oxidation of diesel exhaust in a smog chamber, Environmental Science and Technology, 41, 6969–6975, doi:10.1021/es070193r, 2007.

Atmos. Chem. Phys. Discuss., doi:10.5194/acp-2017-44, 2017
Manuscript under review for journal Atmos. Chem. Phys.
Discussion started: 8 February 2017

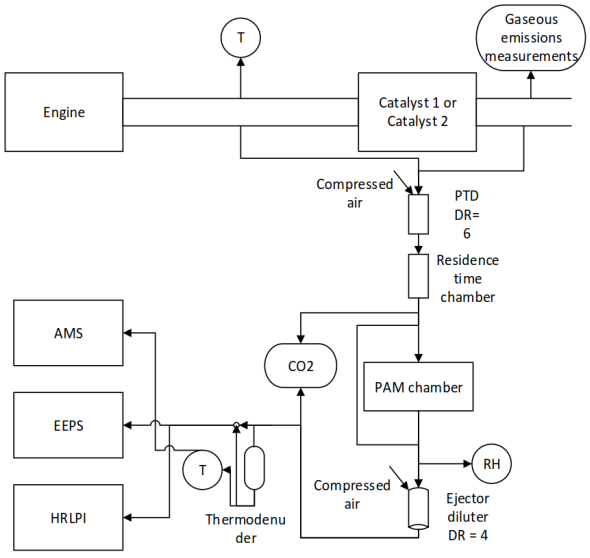

Figure 1. A schematic picture of the measurement setup.

Atmos. Chem. Phys. Discuss., doi:10.5194/acp-2017-44, 2017
Manuscript under review for journal Atmos. Chem. Phys.
Discussion started: 8 February 2017

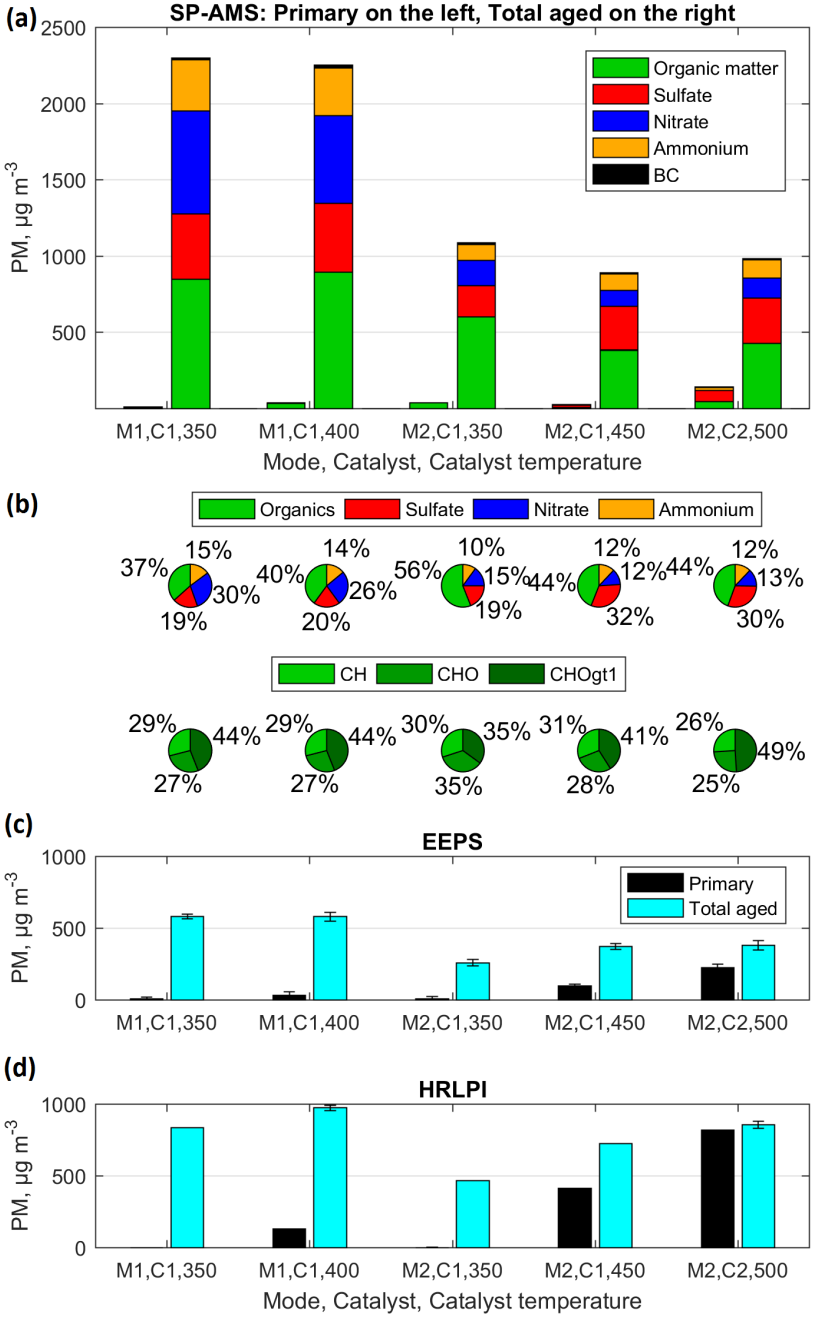

Figure 2. Exhaust primary and total aged particle mass concentrations measured by (a) SP-AMS, (c) EEPS and (d) HRLPI at different engine modes and catalyst temperatures. All values have bean corrected by dilution ratio used in the sampling system. Secondary particle mass can be calculated by subtracting primary from total aged emission. The composition of the total aged particulate matter and the organic particulate matter is presented as pie charts (b). The fraction of black carbon is less or equal to 1 % and therefore left out from the pie charts.

Atmos. Chem. Phys. Discuss., doi:10.5194/acp-2017-44, 2017
Manuscript under review for journal Atmos. Chem. Phys.
Discussion started: 8 February 2017

Atmospheric Chemistry and Physics Discussions

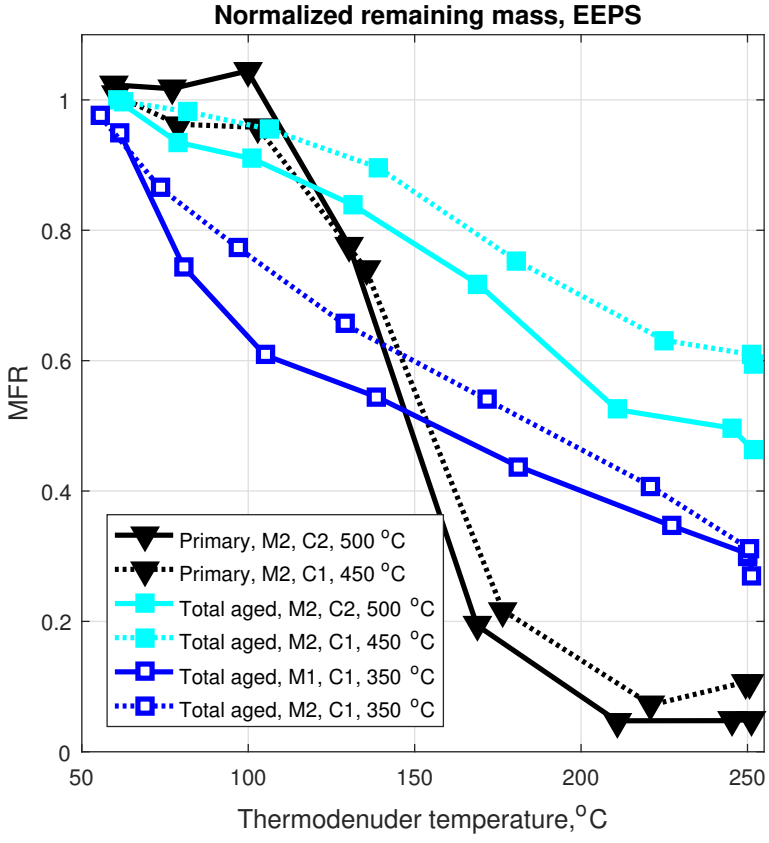

Figure 3. Results of particle volatility measurements. Particle mass fraction remaining (MFR) after the thermodenuder treatment for the exhaust aerosol sample of three different types of particle emission from the natural gas engine. MFR values were calculated from the size distributions measured by EEPS with unit mass assumption.

Atmos. Chem. Phys. Discuss., doi:10.5194/acp-2017-44, 2017
Manuscript under review for journal Atmos. Chem. Phys.
Discussion started: 8 February 2017

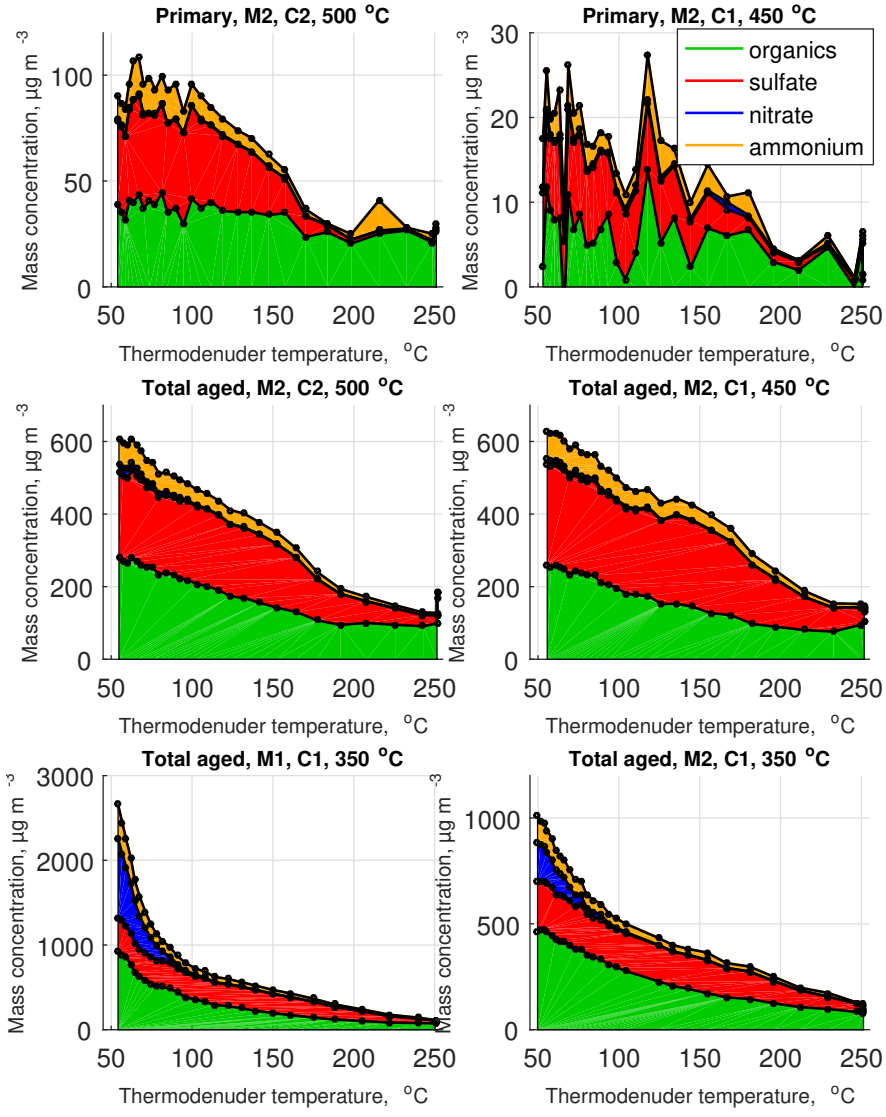

Figure 4. Concentration of different chemical compounds of particles remaining after the thermodenuder treatment conducted for the exhaust aerosol. The mass concentrations were measured using the SP-AMS at different thermodenuder temperatures and corrected by the dilution ratio used in the sampling system.

Atmos. Chem. Phys. Discuss., doi:10.5194/acp-2017-44, 2017
Manuscript under review for journal Atmos. Chem. Phys.
Discussion started: 8 February 2017

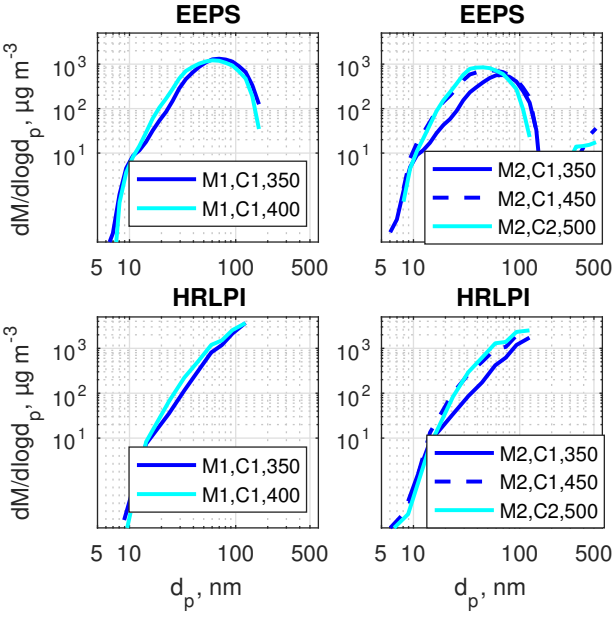

Figure 5. Particle mass size distributions measured by EEPS and HRLPI and corrected by the dilution ratios. Cases M1, C1 on the left, and cases M2, C1 and M2, C2 on the right. Cyan curves stand for the higher catalyst temperatures and blue for the lower ones.

Atmos. Chem. Phys. Discuss., doi:10.5194/acp-2017-44, 2017
Manuscript under review for journal Atmos. Chem. Phys.
Discussion started: 8 February 2017

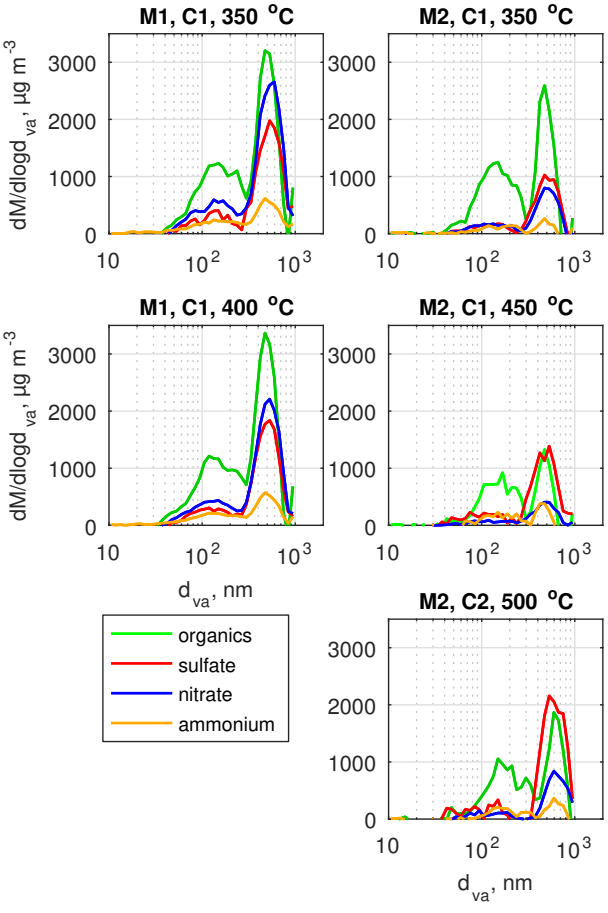

Figure 6. Component-wise particle mass size distributions measured by SP-AMS and corrected by the dilution ratios.

Atmos. Chem. Phys. Discuss., doi:10.5194/acp-2017-44, 2017
Manuscript under review for journal Atmos. Chem. Phys.
Discussion started: 8 February 2017

Atmospheric Chemistry and Physics Discussions

Table 1. (a): Particle mass concentrations of primary and total aged particles (SP-AMS), increase of particle mass (%) in PAM chamber, calculated atmospheric ages simulated by PAM chamber and O/C ratios measured by SP-AMS. If no increase in PAM is presented, it is larger than 100 000 %. (b): The particle mass of species (SP-AMS) in all cases and are also presented in the table as well as (c): the concentrations of gaseous emissions (published already in Lehtoranta et al. (2016)). Values have been corrected by the dilution ratio used in the sampling system.

(a)	M1, C1, 350 °C	M1, C1, 400 °C	M2, C1, 350 °C	M2, C1, 450 °C	M2, C2, 500 °C
Primary PM, μg m^{-3}, SP-AMS	12	40	40	27	141
Total aged PM, μ g m^{-3}, SP-AMS	2299	2253	1089	890	986
Increase in PAM, %, SP-AMS	18400	5560	2620	3190	598
Increase in PAM, %, EEPS	7130	1660	2680	278	69
Increase in PAM, %, HRLPI	-	643	22800	75	4
Atmospheric age, days	10.0	10.7	4.6	4.7	9.3
O/C	1	1.1	1	0.9	1.2
(b): Total aged PM of species, μ g m^{-3}, SP-AMS					
Organic	849	894	602	387	429
Sulfate	427	452	205	286	297
Nitrate	675	577	163	104	129
Ammonium	335	313	107	109	122
(c): Concentrations of gaseous emissions, ppm					
NO	3	4	3	12	4
CO	14	7	14	8	4
Methane	906 ± 16	904 ± 30	2232 ± 74	2238 ± 51	1360 ± 7
Ethane	18	17	68	49	15
Propane	1	1	21	6	1
Ethene	0	0	2	0	0

Atmos. Chem. Phys. Discuss., doi:10.5194/acp-2017-44, 2017
Manuscript under review for journal Atmos. Chem. Phys.
Discussion started: 8 February 2017

Atmospheric Chemistry and Physics Discussions

Table 2. SOA production factors calculated from the SP-AMS data in this study, and in literature (Age = OH-exposure/ ($1.5 * 10^6$ molecules cm^{-3})). *Calculated assuming gasoline density 0.75 kg l^{-1} and consumption 7.9 l (100 km)$^{-1}$.

Source	Age	PF (mg kg_{fuel}^{-1})	Reference
NG engine:			
M1, C1, 350 °C	10 days	17	This study
M1, C1, 400 °C	10.7 days	18	This study
M2, C1, 350 °C	4.6 days	12	This study
M2, C1, 450 °C	4.7 days	8	This study
M2, C2, 500 °C	9.3 days	8	This study
Gasoline vehicle, parts of NEDC cycle	~1-8 days	7-155 *	Karjalainen et al. (2016)
Vehicle fleet in highway tunnel	5.4 days	350	Tkacik et al. (2014)
Gasoline vehicle, hot start	3 h	13.8	Gordon et al. (2014a)
Gasoline vehicle, cold start	3 h	19-60	Gordon et al. (2014a)
Gasoline vehicles, idling	3-6 h	5-90	Nordin et al. (2013)
Gasoline vehicles, cold start	Unknown	480	Nordin et al. (2013)
Gasoline vehicle, NEDC cycle	8 h	345	Platt et al. (2013)
Small 2-stroke off-road engine	1-7 h	240-1400	Gordon et al. (2013)
Small 4-stroke off-road engine	1 h	100-130	Gordon et al. (2013)
Diesel vehicle, deactivated catalyst	Unknown	230-560	Chirico et al. (2010)
Diesel vehicle, catalyst working	Unknown	12-20	Chirico et al. (2010)

Atmos. Chem. Phys. Discuss., doi:10.5194/acp-2017-44, 2017
Manuscript under review for journal Atmos. Chem. Phys.
Discussion started: 8 February 2017

Atmospheric Chemistry and Physics Discussions

Table 3. The temperatures where 50 % of the volatile fraction of species has evaporated.

$T_{volatile,\ 50\ \%}$ (°C)	Primary M2, C2,500 °C	Primary M2, C1, 450 °C	Total aged M2, C2, 500 °C	Total aged M2, C1, 450 °C	Total aged M1, C1, 350 °C	Total aged M2, C1, 350 °C
Organics	98	-	119	123	84	104
Sulfate	145	-	172	187	162	185
Nitrate	82	-	81	91	65	65
Ammonium	100	-	135	151	70	79